AIP | Applied Physics Letters

Direct observation of guided-mode interference in polymer-loaded plasmonic waveguide

Q. Q. Cheng, T. Li, R. Y. Guo, L. Li, S. M. Wang et al.

Citation: Appl. Phys. Lett. **101**, 171116 (2012); doi: 10.1063/1.4764116
View online: http://dx.doi.org/10.1063/1.4764116
View Table of Contents: http://apl.aip.org/resource/1/APPLAB/v101/i17
Published by the American Institute of Physics.

Direct observation of guided-mode interference in polymer-loaded plasmonic waveguide

Q. Q. Cheng, T. Li,[a] R. Y. Guo, L. Li, S. M. Wang, and S. N. Zhu
National Laboratory of Solid State Microstructures, College of Engineering and Applied Sciences, School of Physics, Nanjing University, Nanjing 210093, China

(Received 19 September 2012; accepted 12 October 2012; published online 25 October 2012)

We report a direct observation of guided-mode interference in polymer-loaded plasmonic waveguides by the technique of leakage radiation microscopy (LRM). Spatial beating patterns of the interferences were clearly characterized with respect to different structural parameters, and the interference properties were analyzed in detail. Besides, the capability of LRM for characterizing the multiple modes was also discussed extensively. Our finding not only offers an efficient technique in analyzing the guided modes and their interference, but also provides a definite guideline in evaluating the validity of LRM and deepens further studies on the dielectric-loaded hybrid waveguide system. © *2012 American Institute of Physics*. [http://dx.doi.org/10.1063/1.4764116]

Plasmonic waveguide, as an important element for the subwavelength integration, always suffers from its large metallic loss. In recent years, dielectric-loaded plasmonic waveguides has received increasing attention due to its capability of optimally balancing the strong field confinement and low propagation loss.[1–5] Moreover, they can be upgraded to active systems by employing the active media (e.g., semiconductors,[6,7] quantum dot or dye-doped polymers,[8–14] nonlinear crystals,[15] etc.), which are helpful in compensating the loss and even amplifying the surface plasmon polariton (SPP). In this regard, metal/dielectric hybrid waveguide offers new freedom to tailor the optical mode in a confined dimension, where the higher ordered modes can also be carefully tailored and taken usage of. Therefore, it is important to analyze the property of those higher ordered modes that possibly exist in hybrid plasmonic waveguide. However, the guided mode characterization is always a difficult issue due to the confined nature, though several approaches has been developed in the last decade.[16–18] Recently, a powerful technique called leakage radiation microscopy (LRM) was developed to analyze not only the SPPs on pure metal surface[19–21] but also the SPPs[22] and guided modes[23–25] in dielectric-loaded waveguides.

In this paper, we report a direct observation of guided-mode interference by LRM in polymer-loaded plasmonic planar waveguides. Obvious spatial beating patterns are clearly captured by the LRM camera, which are almost independent to the grating couplers for a fixed polymer layer thickness, indicating the intrinsic property of the supported guided modes. The beating performance as well as the interference property is analyzed concerning on different structural parameters and polarizations. In addition, the capability of LRM in analyzing guided modes in this hybrid plasmonic system is discussed, which offers a guideline for exact usage of LRM in characterizing the multiple modes.

Figure 1 schematically shows the design of the polymer-loaded planar waveguide. Here, the polymer is a kind of photoresist (AR-P 3110), which does not react under the illumination of the used laser of $\lambda_0 = 633\,\text{nm}$ (He-Ne laser). In experiments, thin silver film is sputtered on a quartz substrate, and followed with a focus ion beam (Strata FIB 201, FEI Company, 30 KeV, 11 pA) milling to fabricate gratings for launching the incident laser to SPP/guided modes. Afterwards, the whole device is spin-coated with a polymer layer, whose thickness can be adjusted by concentration of photoresist and the spin rate.

Before getting into detailed experimental results, we would first analyze the mode properties. According to the experimental condition, we assume the thickness of polymer layer varies and that of silver layer is fixed at $t = 60\,\text{nm}$. Since t is much larger than the skin depth of silver, we consider this structure approximately to be an insulator-insulator-metal (I/I/M) trilayer system with its mode equation as[26]

$$h\sqrt{k_0^2 n_2^2 - \beta^2} = m\pi + \arctan\left(f_1\sqrt{\frac{\beta^2 - k_0^2 n_1^2}{k_0^2 n_2^2 - \beta^2}}\right) + \arctan\left(f_3\sqrt{\frac{\beta^2 - k_0^2 n_3^2}{k_0^2 n_2^2 - \beta^2}}\right), \quad (1)$$

where k_0 is the free-space wave vector, β is the in-plane wave vector of the considered modes, h is the thickness of the polymer layer, and m indicates the order of modes. Parameters of n_1, n_2, and n_3 correspond to the refractive index of silver, polymer, and air, respectively. For TM polarization, $f_1 = (n_2/n_1)^2$ and $f_3 = (n_2/n_3)^2$; while for TE polarization, $f_1 = f_3 = 1$. By solving the dispersion relation of Eq. (1), we can easily obtain the effective index of series of TM and TE modes with respect to different thickness of polymer layer (h). At experimental wavelength ($\lambda_0 = 633\,\text{nm}$), the refractive index of quartz substrate, silver, polymer, and air are 1.545, 0.0554 + 4.2434i,[27] 1.62, and 1, respectively. Figure 2(a) depicts the calculated result, which reveals similar mode diagram as reported previously,[23] in which two green lines label out two effective indices (1.32 and 1.25) corresponding to the numerical apertures (NA) of two oil-immersed objectives used in the LRM characterizations. It

[a]Author to whom correspondence should be addressed. Electronic mail: taoli@nju.edu.cn. URL: http://dsl.nju.edu.cn/litao.

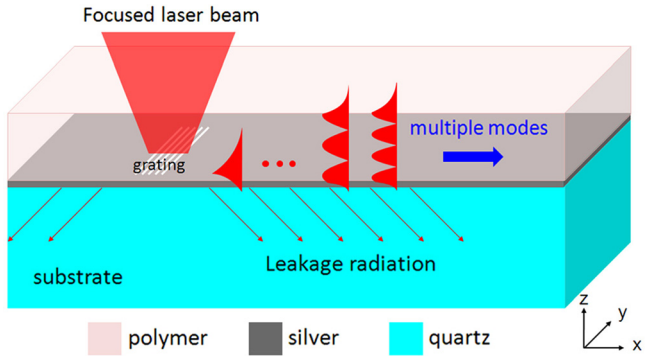

FIG. 1. Schematics of polymer-loaded hybrid plasmonic waveguide, where multiple modes are launched by a grating in the silver film from an incident laser beam.

should be noted that only the modes with effective indices lower than the NA of objective can be detected by the LRM. For example, only TM_2 mode will be observed in the case of $h = 560$ nm, as indicated by the vertical blue guideline. Figure 2(b) further depicts the mode profiles (E_x) of the TM_3 and TM_4 in comparison with the TM_0 (SPP mode) in the case of $h = 1\ \mu$m, which will be particularly investigated in experiments. Another mode within the achievable range is TE_3 whose field intensity penetrated into the metal layer is much weaker than those of TM ones. So, it would be almost invisible in the LRM detection, which will be confirmed by our experiments.

In experiments, two series samples were fabricated with $h = 1\ \mu$m and 560 nm, respectively. For the $h = 1\ \mu$m series, the period of coupling grating changes from 500 nm to 620 nm, in order to investigate the property of couple-in modes. Figure 3(a) shows the detected (NA = 1.32) mode propagation on the sample with the grating of P = 550 nm with a TM-polarized incidence. Very clear interference fringes are observed in the field intensity, which is also manifested as periodic oscillation in the retrieved data shown in Fig. 3(b). We further made a Fourier transformation (FT) on this field distribution numerically and found a distinct reciprocal peak of $\Lambda = 2.52\ \mu m^{-1}$ [see Fig. 3(c)], corresponding to a spatial period of 2.50 μm. Although there have been some studies shown that fringes may appear in LRM detection due to the interference of leakage wave of SPP and a background scattering limited by the NA of objective,[28] this observed field oscillating intensity is much stronger than the

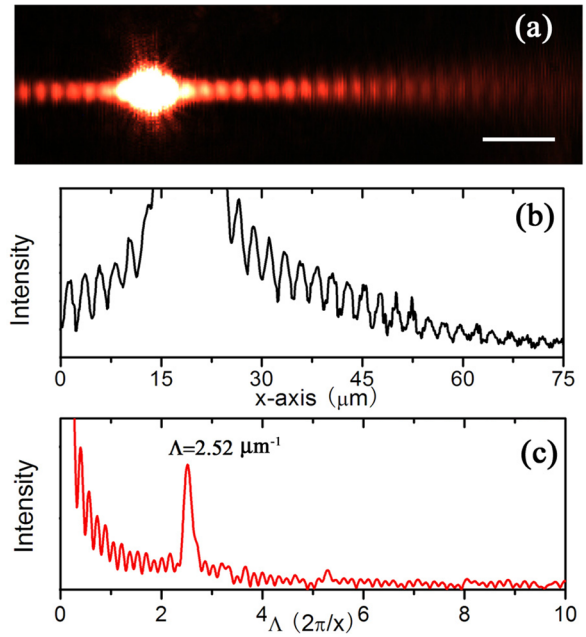

FIG. 3. (a) LRM (NA = 1.32) detected mode propagation of the sample with $h = 1\ \mu$m and coupling grating P = 550 nm (scale bar = 10 μm). (b) Field intensity data in mode propagations retrieved from the map (a). (c) Spatial Fourier spectrum of the field distribution, where a distinct peak is revealed with $\Lambda = 2.52\ \mu m^{-1}$.

reported ones. And common SPP (TM_0) interference, which would be detected in small h cases,[22] should not be detected here due to the large k vectors for this $h = 1\ \mu$m case. So, this strong spatial beat appears a little bit surprising.

Let us refer to the mode diagram in Fig. 2(a), two TM modes (TM_3 and TM_4) are found within the LRM achievable region ($1 < n < 1.32$), whose wave vectors (k_x) are 1.27 $\times (2\pi/\lambda_0)$ and 1.02 $\times (2\pi/\lambda_0)$, respectively, corresponding to wavelengths of $\lambda_{TM3} = 498$ nm and $\lambda_{TM4} = 620$ nm. It is very possible that these two modes were simultaneously launched by the grating of P = 550 nm, resulting in this interference beat. According to $k_{beat} = k_1 - k_2$, we calculated the period of beat is 2.53 μm, agreeing well with the experimental result (2.50 μm). Therefore, it is evident that the observed spatial beat comes from the interference of two guided modes (TM_3 and TM_4) with different wave numbers, which is rather different from the reported SPP standing wave arising from interference of two opposite-directional propagating SPP beam with same wave numbers.[22]

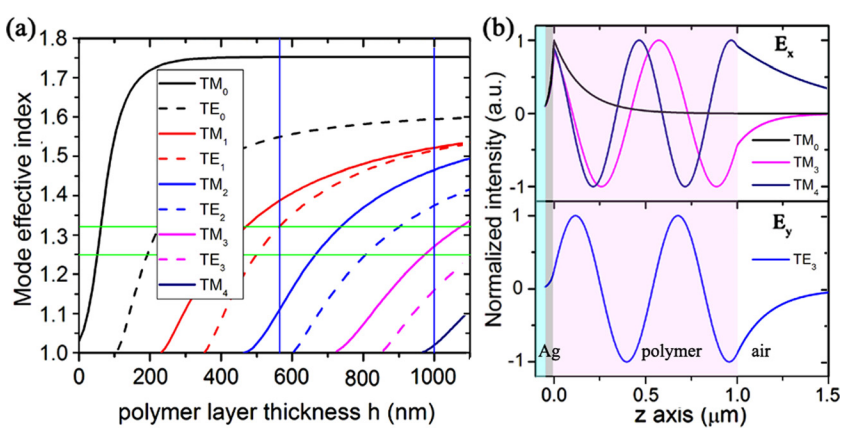

FIG. 2. (a) Calculated mode effective index of polymer-loaded waveguide with respect to different polymer layer thickness including all TM and TE modes. (b) Mode profiles of TM3, TM_4, and TE_3 (achievable within the range of NA < 1.32 for $h = 1\ \mu$m case) with the comparison with the TM_0 (SPP) mode.

From the mode profiles, we also find the reason why the higher ordered TM modes can be detected by LRM, since these higher ordered TM modes also have strong E_x intensities at the metal/polymer interface just like the SPPs, which can penetrate through the metal layer and leak out to be detected. It should be mentioned here that although different ordered modes inside a waveguide should be orthogonal and the overlap integration of field should be zero, the E_x intensity at the metal/polymer interface is determined to be maxima and strongly interfered. This particular TM mode property of such kind of hybrid plasmonic waveguide is a critical condition for this interference beat to be detected, which may not be achievable in conventional dielectric waveguides. Moreover, the interference is a coherent process, so it will not occur in luminescent guided mode in dye-doped PMMA waveguides.[25] On the contrary, the characteristic of TE mode determines the field intensity decays to be very small at the metal/polymer interface [see Fig. 2(b)], which greatly inhibits the LRM detection.

Next, we investigate the influence of the launching gratings with various periods. In principle, only when a matched reciprocal vector is provided, the incident laser beam can be efficiently coupled into the SPP or guided modes. However, our experimental results show that all different gratings ($P = 500$, 540, 580, 620 nm) are able to launch the modes with apparent interference patterns, as shown in Figs. 4(a)–4(d). It is mainly due to the broad line width of the coupling process that covers a wide k-vector range. Nevertheless, by carefully checking these interference patterns, one may find these interference intensities are not equivalent, which is revealed more obviously in their Fourier spectra, as shown in Fig. 4(e). It is found that intermediate ones ($P = 540$ and 550 nm) are stronger that others, despite they almost have same peak position ($\Lambda \sim 2.52\ \mu m^{-1}$). It indicates that two concerned TM modes ($\lambda_{TM3} = 498$ nm and $\lambda_{TM4} = 620$ nm) can be launched more equivalently by the intermediate grating and lead to the strongest interference. In a common consideration, there would be no beating pattern if only one pure mode is excited, for example, the sample of $P = 620$ nm, designed for the mode TM_4. However, interference beat is still clearly manifested though it is worse than the strongest one [see Fig. 4(e)]. Besides the reason of the finite line-width coupling process as has been mentioned, another explanation of this phenomenon is that there may be a number of defects inside the hybrid waveguide that will diffract the pure mode to other ones as the modes propagate. It is also confirmed by our simulations (not shown here).

This interference of mode-TM_3 and TM_4 is further confirmed by alternating the LRM objective and polymer thickness. Figure 5(a) is the result from the same sample of the $P = 550$ nm (shown in Fig. 3) but detected by another objective of $NA = 1.25$. No beating pattern is observed, because there is only TM_4 locates within the range of $1 < n < 1.25$. Similar results were obtained in the case of thinner polymer thickness ($h = 560$ nm). There is only TM_2 detected by LRM system both for cases of $NA = 1.32$ [Fig. 5(b)] and 1.25 [Fig. 5(c)]. It further confirms that the previous reported interference fringes due to the LRM setup[28] did not obviously take place here. So, it should be stressed that although there are no spatial beat observed in Figs. 5(a)–5(c), mode interference still factually exists if two or more modes are excited simultaneously.

In addition, a TE polarized incidence was introduced in the same system. As predicted, no obvious propagation is detected by the LRM, as shown in Fig. 5(d), due to the weak electric field of TE mode at the interface. However, it does not mean that there is no TE mode launched by the coupling grating. To prove it, we intentionally introduced another grating in the propagation path of the guided mode, and strong scattered signal was detected from this couple-out grating (50 μm away from the source), as shown in Fig. 5(d). It indicates that considerable TE mode is launched by the couple-in grating. Actually, those lower ordered TM modes beyond the range of NA of LRM, including the lowest one (SPP mode), would have the similar behavior, whose propagations cannot be directly imaged by the LRM but can be scattered out by additional gratings.

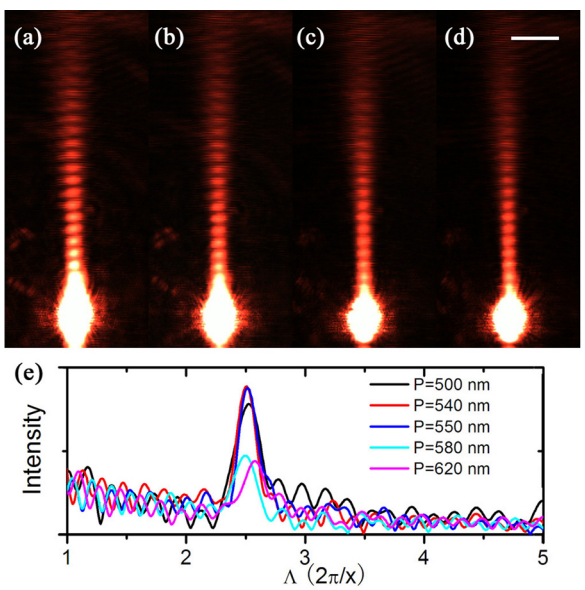

FIG. 4. LRM ($NA = 1.32$) detected mode interference with for different coupling grating samples: (a) $P = 500$ nm, (b) 540 nm, (c) 580 nm, and (d) 620 nm, where scale bar = 10 μm. (e) Fourier spectra of field distribution of these samples.

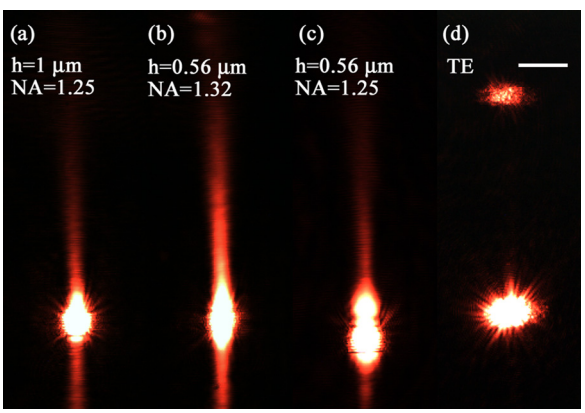

FIG. 5. LRM detected mode propagations of (a) $NA = 1.25$ for sample $h = 1$ μm, (b) $NA = 1.32$, and (c) 1.25 for sample $h = 560$ nm (TM-polarized incidence), and the result of (d) a TE-polarized incidence with the same structural parameters of Fig. 3(a) (scale bar = 10 μm).

In summary, we presented direct observation of multimode interference in a hybrid plasmonic waveguide using LRM. From our results, it is definitely concluded that the observed spatial beat comes from two higher TM modes, which were simultaneously launched by a single grating with a loose excitation condition. We also found this interfere appearance is affected by NA of LRM objective, and the LRM cannot image the TE guided mode howbeit it can be launched as well. Our results provide an efficient technique in investigating guided modes in dielectric-loaded plasmonic waveguide, and verify the validity range of the LRM in mode characterization. Our findings are further expected to guide the powerful LRM technique to be applied appropriately in a broader region in plasmonic wave guide system.

This work was supported by the State Key Program for Basic Research of China (Nos. 2012CB921501, 2010CB630703, 2009CB930501, and 2011CBA00200), the National Natural Science Foundation of China (Nos. 10974090, 11174136, 11021403, and 60990320), and PAPD of Jiangsu Higher Education Institutions.

[1]T. Holmgaard and S. I. Bozhevolnyi, Phys. Rev. B **75**, 245405 (2007).
[2]R. F. Oulton, V. J. Sorger, D. A. Genov, D. F. P. Pile, and X. Zhang, Nat. Photonics **2**, 496 (2008).
[3]V. J. Sorger, Z. L. Ye, R. F. Oulton, Y. Wang, G. Bartal, X. B. Yin, and X. Zhang, Nat. Commun. **2**, 331 (2011).
[4]A. V. Krasavin and A. V. Zayats, Opt. Express **18**, 11791 (2010).
[5]S. A. Maier and H. A. Atwater, J. Appl. Phys. **98**, 011101 (2005).
[6]M. Z. Alam, J. Meier, J. S. Aitchison, and M. Mojahedi, Opt. Express **15**, 176 (2007).
[7]C. Sirtori, C. Gmachl, F. Capasso, J. Faist, D. L. Sivco, A. L. Hutchinson, and A. Y. Cho, Opt. Lett. **23**, 1366 (1998).
[8]I. De Leon and P. Berini, Nat. Photonics **4**, 382 (2010).
[9]A. Banerjee, R. Li, and H. Grebel, Appl. Phys. Lett. **95**, 251106 (2009).
[10]M. Nezhad, K. Tetz, and Y. Fainman, Opt. Express **12**, 4072 (2004).
[11]J. Seidel, S. Grafström, and L. Eng, Phys. Rev. Lett. **94**, 177401 (2005).
[12]P. M. Bolger, W. Dickson, A. V. Krasavin, L. Liebscher, S. G. Hickey, D. V. Skryabin, and A. V. Zayats, Opt. Lett. **35**, 1197 (2010).
[13]M. A. Noginov, G. Zhu, M. Mayy, B. A. Ritzo, N. Noginova, and V. A. Podolskiy, Phys. Rev. Lett. **101**, 226806 (2008).
[14]M. A. Noginov, V. A. Podolskiy, G. Zhu, M. Mayy, M. Bahoura, J. A. Adegoke, B. A. Ritzo, and K. Reynolds, Opt. Express **16**, 1385 (2008).
[15]F. F. Lu, T. Li, J. Xu, Z. D. Xie, L. Li, S. N. Zhu, and Y. Y. Zhu, Opt. Express **19**, 2858 (2011).
[16]H. Ditlbacher, J. R. Krenn, N. Felidj, B. Lamprecht, G. Schider, M. Salerno, A. Leitner, and F. R. Aussenegg, Appl. Phys. Lett. **80**, 404 (2002).
[17]T. Holmgaard, Z. Chen, S. I. Bozhevolnyi, L. Markey, and A. Dereux, Opt. Express **17**, 2968 (2009).
[18]A. L. Campillo, J. W. P. Hsu, K. R. Parameswaran, and M. M. Fejer, "Direct imaging of multimode interference in achannel waveguide," Opt. Lett. **28**, 399 (2003).
[19]A. Drezet, A. Hohenau, A. L. Stepanov, H. Ditlbacher, B. Steinberger, N. Galler, F. R. Aussenegg, A. Leitner, and J. R. Krenn, Appl. Phys. Lett. **89**, 091117 (2006).
[20]L. Li, T. Li, S. M. Wang, C. Zhang, and S. N. Zhu, Phys. Rev. Lett. **107**, 126804 (2011).
[21]L. Li, T. Li, S. M. Wang, S. N. Zhu, and X. Zhang, Nano Lett. **11**, 4357 (2011).
[22]L. Grave de Peralta and D. Domínguez, "SPP tomography experiments with surface plasmon polariton standing waves," Opt. Commun. (in press).
[23]D. G. Zhang, X. C. Yuan, G. H. Yuan, P. Wang, and H. Ming, J. Opt. **12**, 035002 (2010).
[24]D. G. Zhang, X. C. Yuan, and J. H. Teng, Appl. Phys. Lett. **97**, 231117 (2010).
[25]D. G. Zhang, Q. Fu, X. X. Wang, Y. K. Chen, P. Wang, and H. Ming, J. Opt. **14**, 015003 (2012).
[26]G. Lifante, *Integrated Photonics: Fundamentals* (Wiley, England, 2003).
[27]P. B. Johnson and R. W. Christy, Phys. Rev. B. **6**, 4370 (1972).
[28]A. Hohenau, J. R. Krenn, A. Drezet, O. Mollet, S. Huant, C. Genet, B. Stein, and T. W. Ebbesen, Opt. Express **19**, 25749 (2011).